Biochimica et Biophysica Acta 1850 (2015) 178–185

Contents lists available at ScienceDirect

Biochimica et Biophysica Acta

journal homepage: www.elsevier.com/locate/bbagen

Astaxanthin prevents TGFβ1-induced pro-fibrogenic gene expression by inhibiting Smad3 activation in hepatic stellate cells

Yue Yang, Bohkyung Kim, Young-Ki Park, Sung I. Koo, Ji-Young Lee *

Department of Nutritional Sciences, University of Connecticut, Storrs, CT 06269, USA

ARTICLE INFO

Article history:
Received 12 May 2014
Received in revised form 3 October 2014
Accepted 14 October 2014
Available online 23 October 2014

Keywords:
Astaxanthin
Non-alcoholic steatohepatitis
Liver fibrosis
Hepatic stellate cell
Transforming growth factor β1
Smad3

ABSTRACT

Background: Non-alcoholic steatohepatitis (NASH) is a subset of non-alcoholic fatty liver disease, the most common chronic liver disease in the U.S. Fibrosis, a common feature of NASH, results from the dysregulation of fibrogenesis in hepatic stellate cells (HSCs). In this study, we investigated whether astaxanthin (ASTX), a xanthophyll carotenoid, can inhibit fibrogenic effects of transforming growth factor β1 (TGFβ1), a key fibrogenic cytokine, in HSCs.
Methods: Reactive oxygen species (ROS) accumulation was measured in LX-2, an immortalized human HSC cell line. Quantitative realtime PCR, Western blot, immunocytochemical analysis, and in-cell Western blot were performed to determine mRNA and protein of fibrogenic genes, and the activation of Smad3 in TGFβ1-activated LX-2 cells and primary mouse HSCs.
Results: In LX-2 cells, ROS accumulation induced by tert-butyl hydrogen peroxide and TGFβ1 was abolished by ASTX. ASTX significantly decreased TGFβ1-induced α-smooth muscle actin (α-SMA) and procollagen type 1, alpha 1 (Col1A1) mRNA as well as α-SMA protein levels. Knockdown of Smad3 showed the significant role of Smad3 in the expression of α-SMA and Col1A1, but not TGFβ1, in LX-2 cells. ASTX attenuated TGFβ1-induced Smad3 phosphorylation and nuclear translocation with a concomitant inhibition of Smad3, Smad7, TGFβ receptor I (TβRI), and TβRII expression. The inhibitory effect of ASTX on HSC activation was confirmed in primary mouse HSCs as evidenced by decreased mRNA and protein levels of α-SMA during activation.
Conclusion: Taken together, ASTX exerted anti-fibrogenic effects by blocking TGFβ1-signaling, consequently inhibiting the activation of Smad3 pathway in HSCs.
General significance: This study suggests that ASTX may be used as a preventive/therapeutic agent to prevent hepatic fibrosis.

1. Introduction

Incidence of non-alcoholic fatty liver disease (NAFLD), the most common cause of chronic liver diseases in the developed countries, has been rapidly increasing in parallel with an obesity epidemic [1–3]. Non-alcoholic steatohepatitis (NASH) is an advanced form of NAFLD, characterized by macrovesicular steatosis, ballooning hepatocytes, apoptotic cells, the presence of Mallory hyaline and/or megamitochondria in the hepatocyte cytoplasm, infiltration of inflammatory cells, and varying stages of fibrosis [4–8]. Fibrosis can slowly advance to cirrhosis, which is an irreversible condition leading to liver failure and increased mortality [9,10].

Activation of hepatic stellate cells (HSCs) is primarily responsible for the production of extracellular matrix and fibrosis development in the liver [11]. During liver injury, quiescent HSCs are activated by fibrogenic cytokines or stimulants, such as transforming growth factor β1 (TGFβ1), platelet derived growth factor and tumor necrosis factor α, as well as lipid peroxides generated by hepatocytes, HSCs, Kupffer cells and platelets [12,13]. In particular, TGFβ1 is the most potent pro-fibrogenic cytokine and its levels are elevated in hepatic fibrosis of animals and humans [14]. TGFβ1 signal is transduced by sequential activation of its two serine/threonine kinase receptors, i.e., TGFβ type II receptor (TβRII) and TGFβ type I receptor (TβRI), which in turn phosphorylates Smad2 or Smad3 for nuclear translocation [15]. It is known that Smad3 regulates transcription of fibrogenic genes, such as α-smooth muscle actin (α-SMA) and procollagen type 1, alpha 1 (Col1A1), which is important for the production of extracellular matrix to repair damaged tissues [16]. Therefore, inhibition of TGFβ1 signaling in HSCs is a major therapeutic target for preventing the initiation and progression of hepatic fibrosis.

Abbreviations: α-SMA, α-smooth muscle actin; ASTX, astaxanthin; BCA, bicinchoninic acid; CEBPβ, CCAAT/enhancer binding protein β; Col1A1, procollagen type I, alpha 1; HSC, hepatic stellate cell; KLF, Krüppel-like factors; NAFLD, non-alcoholic fatty liver disease; NASH, non-alcoholic steatohepatitis; NFκB, nuclear factor kappa B; NOX4, NADPH oxidase 4; qRT-PCR, quantitative realtime PCR; ROS, reactive oxygen species; siRNA, small interference RNA; Sp1, specificity protein 1; tBHP, tert-butyl hydrogen peroxide; TβRI, TGFβ type I receptor; TβRII, TGFβ type II receptor; TGFβ1, transforming growth factor β1

* Corresponding author. Tel.: +1 860 486 1827; fax: +1 860 486 3674.
E-mail address: ji-young.lee@uconn.edu (J.-Y. Lee).

http://dx.doi.org/10.1016/j.bbagen.2014.10.014
0304-4165/

Astaxanthin (ASTX) is a xanthophyll carotenoid, which gives reddish appearance to aquatic animals such as salmon and shrimp [17]. Due to its unique structure containing hydroxyl and keto moieties on both ends of its polyene chain, ASTX has a strong antioxidant activity [18]. Studies have demonstrated that ASTX exerts protective effects against oxidative stress [19,20], inflammation [21,22], type 2 diabetes [23], and cardiovascular diseases [24]. Our previous study demonstrated that ASTX lowered plasma lipid levels and enhanced hepatic antioxidant capacity in apolipoprotein E knockout mice [25]. However, whether ASTX can prevent the development of liver fibrosis has never been addressed. In this study, we aimed to investigate the role of ASTX in the regulation of fibrogenic genes in HSCs using both a human HSC cell line and primary mouse HSCs. Our study presents the first evidence that ASTX inhibits TGFβ1-induced Smad3 activation, consequently repressing the expression of fibrogenic genes.

2. Materials and methods

2.1. Isolation of primary mouse HSCs

Primary HSCs were isolated from C57BL/6J mouse liver using the collagenase/pronase digestion method [26]. In brief, mice were anesthetized with ketamine/xylazine (120/6 mpk) (Butler Schein, Dublin, OH). Abdominal and chest cavities were opened to expose the portal vein and to locate the heart and vena cava, respectively. Subsequently, a 20G × 1" I.V. catheter (Terumo, Somerset, NJ) was inserted into the vena cava through the right atrium and the portal vein was cut. A mouse liver was perfused at 5 mL/min with 25 mL SC-1 solution consisting of the following (per L); 8000 mg NaCl, 400 mg KCl, 88.17 mg NaH_2PO_4 $2H_2O$, 120.45 mg Na_2HPO_4 $12H_2O$, 2380 mg 4-(2-hydroxyethyl)-1-piperazineethanesulfonic acid (HEPES), 350 mg $NaHCO_3$, 190 mg ethylene glycol tetraacetic acid, and 900 mg glucose, pH 7.2–7.3 [27]. The liver was, then, digested with 300 μg/mL pronase E (Roche, Mannheim, Germany) in SC-2 solution consisting of 8000 mg NaCl, 400 mg KCl, 88.17 mg NaH_2PO_4 $2H_2O$, 120.45 mg Na_2HPO_4 $12H_2O$, 2380 mg HEPES, 350 mg $NaHCO_3$, and 560 mg $CaCl_2$ $2H_2O$, per L, pH 7.2–7.3 [27], followed by 600 μg/mL collagenase D (Roche, Mannheim, Germany) in SC-2 solution at 5 mL/min for 5 min each. The digested liver was harvested and filtered through a 100 μm cell strainer (Fisher Scientific, Pittsburgh, PA). The hepatic cells were then centrifuged at 60 × g for 1 min to separate non-parenchymal cells from hepatocytes. The supernatant containing non-parenchymal cells was separated based on density using a top layer of Gey's Balanced Salt Solution (GBSS) [28], a middle layer of 10% Nycodenz (Axis-Shield, Scotland) and a bottom layer of 14.5% Nycodenz diluted in GBSS. The tube was centrifuged at 2100 × g or 20 min and the primary HSCs were collected from the interface between the GBSS and 10% Nycodenz.

2.2. HSC culture and treatment

LX-2 cells were kindly provided by Dr. Scott Friedman at the Icahn School of Medicine at Mount Sinai (New York, New York). Cells were maintained in low-glucose DMEM containing 2% FBS, 4 mM L-glutamine, 100 U/mL penicillin and 100 μg/mL streptomycin in a 37 °C humidified cell culture chamber providing 5% CO_2. LX-2 cells were incubated with varying concentrations of ASTX for 12 or 24 h, and subsequently activated by 2 ng/mL of TGFβ1 (Peprotech, Rocky Hill, NJ) for 1 to 24 h. Primary mouse HSCs were plated on untreated petri dishes (BD Falcon, Franklin Lakes, NJ) and maintained in low-glucose DMEM supplemented with 10% FBS, 4 mM L-glutamine, 100 U/mL penicillin and 100 μg/mL streptomycin in a 37 °C humidified cell culture chamber under 5% CO_2. ASTX (25 μM) was added at day 2 or day 4 after plating until day 6 with daily media change. All cell culture supplies were purchased from HyClone (Thermo Scientific, Logan, UT).

ASTX was kindly provided by Fuji Chemical Industry Co., Ltd. (Toyama, Japan). ASTX stock solution (10 mM) was prepared in DMSO and stored at −80 °C until use. Before cell treatments, ASTX stock was incubated in 70 °C for 10 min, after which the ASTX stock was dissolved in FBS and then diluted in cell culture medium to obtained desired concentrations. The final FBS concentration in ASTX-containing medium was 2% and therefore the same amount FBS and DMSO was added to controls. All ASTX-containing solutions were kept in the dark to prevent any light-induced degradation.

2.3. Cytotoxicity test

LX-2 cells were incubated with 0–200 μM ASTX for 24 h and its cytotoxicity was measured using a Cell Counting Kit-8 (Dojindo Inc., Rockville, MD) as previously described [29]. Positive control (0.5 mM SDS) was run in parallel.

2.4. Reactive oxygen species (ROS) measurement

Cellular ROS levels were measured in LX-2 cells as previously described [30]. Briefly, LX-2 cells were plated in a black 24-well plate (Wallac Oy, Turku, Finland). When cells reached ~90% confluency, they were pre-incubated with 5, 10 or 25 μM ASTX for 24 h and subsequently stimulated with 2 ng/mL TGFβ1 or 10 μM tert-butyl hydrogen peroxide (tBHP, Sigma, St. Louis, MO) for additional 24 h. cells were then incubated with 5 μM dichlorofluorescein (Sigma, St. Louis, MO) for 30 min and fluorescence was read at an excitation wavelength of 485 nm and an emission wavelength of 530 nm. The data were expressed as fluorescent intensity per μg of cell protein.

2.5. Quantitative realtime PCR (qRT-PCR)

Total RNA extraction, cDNA synthesis, and qRT-PCR were conducted using a Bio-Rad CFX96 Real-Time system (Bio-Rad, Hercules, CA) as previously described [31,32]. Gene sequences were obtained from the GenBank database and primers were designed using Beacon Designer (Premier Biosoft, Palo Alto, CA). Primer sequences are available in the online supplemental table.

2.6. Western blot analysis

Whole cell lysates were prepared to conduct Western blot as we previously described [32] using antibodies against α-SMA (Sigma, St. Louis, MO), Smad3 (Millipore, Billerica, MA), and phospho-Smad3 (Cell Signaling, Danvers, MA). β-Tubulin (Santa Cruz Biotechnology, Santa Cruz, CA) or β-actin (Sigma, St. Louis, MO) was used as a loading control. For Western blot of nuclear and cytoplasmic cell fractions, the fractions were prepared using a nuclear extraction kit (Cayman, Ann Arbor, MI) as we previously described [33]. Glyceraldehyde 3-phosphate dehydrogenase (GAPDH) (Santa Cruz Biotechnology, Santa Cruz, CA) and lamin B (Santa Cruz Biotechnology) were used as a loading control for cytoplasmic and nuclear fractions, respectively. Blots were developed using Westpico horseradish peroxidase chemiluminescence (Pierce, Rockford, IL) and images were analyzed using a Chemidoc XRS + system (Bio-Rad) and Image Lab software (Bio-Rad).

2.7. Immunocytochemistry

LX-2 cells and primary HSCs were plated on a Millicell EZ slide (Millipore, Billerica, MA). After treatment with ASTX, cells were fixed with 4% formaldehyde for 10 min and subsequently blocked with 1% BSA in 1X TBS containing 0.1% Triton X-100 (TBS-T) for 30 min at room temperature. Fixed cells were then incubated with α-SMA antibody overnight at 4 °C, after which they were incubated with anti-mouse DyLight 488 conjugated secondary antibody (Abcam, Cambridge, MA) in the dark for 1 h at room temperature. Cell nuclei were visualized by DAPI staining (100 ng/mL in PBS) for 10 min. After washing the cells with TBS-T, Prolong Gold anti-fade reagent

(Invitrogen, Grand Island, NY) was added onto the cells and images were taken with an AxioCam MRc camera (Carl Zeiss Microscopy, Jena, Germany).

2.8. In-cell Western

Primary HSCs were incubated on an uncoated μ-Plate (Ibidi, Verona, WI). After 6 days of activation with or without ASTX, HSCs were fixed in 4% formaldehyde for 20 min at room temperature and washed with 1% TBS-T for 5 times for 5 min each. The cells were blocked with Odyssey® Blocking Buffer for 30 min, then incubated with α-SMA primary antibody for 2 h at room temperature. Subsequently, the cells were co-incubated with IRDye 800CW secondary antibody and CellTag 700 stain, a fluorescent stain for cell number normalization, in the dark for 1 h at room temperature. Pictures were taken using an Odyssey CLx Imager (Li-COR, Lincoln, NE) and signals were quantified by a Li-COR Image Studio software with normalization using a signal of CellTag 700 stain. All reagents and imaging tools for In-cell Western were purchased from Li-COR.

2.9. Small interference RNA (siRNA) transfection

LX-2 cells were transfected with either Silencer® Negative Control scrambled siRNA (Ambion, Invitrogen, Grand Island, NY) or siGENOME SMARTpool SMAD3 siRNA (siGenome, Thermo Scientific, Logan, UT) as described previously [34]. Twenty four hours after the transfection, cells were pretreated with 25 μM ASTX for 12 h, after which they were stimulated by 2 ng/mL TGFβ1 for additional 12 h for subsequent qRT-PCR analysis.

2.10. Statistical analysis

One-way analysis of variance (ANOVA) and the Newman Keul pairwise post-hoc test were used to detect significant differences between groups. Statistical analyses were conducted by using GraphPad Prism6 (GraphPad Software, La Jolla, CA). P values less than 0.05 were considered significant and all values were presented as mean ± SEM.

3. Results

3.1. ASTX prevented TGFβ1 and tBHP-induced ROS accumulation in LX-2 cells

We firstly tested ASTX cytotoxicity in LX-2 cells. ASTX showed minimal cytotoxicity in LX-2 cells with more than 90% cell viability up to 25 μM (Fig. 1A). Excessive ROS accumulation has been shown to activate HSCs, which is a key event in the development of hepatic fibrosis [35]. As ASTX is a potent antioxidant [36], we determined if ASTX decreases ROS accumulation induced by TGFβ1 or tBHP in LX-2 cells. Both TGFβ1 and tBHP significantly increased cellular ROS levels, which were attenuated by ASTX (Fig. 1B & C). At 25 μM, ASTX completely abolished the increase in cellular ROS levels induced by TGFβ1 and tBHP.

3.2. ASTX attenuated the TGFβ1-induced expression of fibrogenic genes in LX-2 cells

TGFβ1 is the most potent pro-fibrogenic cytokine in HSCs [14] and therefore we determined the effect of ASTX on TGFβ1-induced fibrogenic response in LX-2 cells. TGFβ1 significantly increased mRNA abundance of α-SMA and Col1A1 as early as 3 h and the mRNA levels reached the highest at 12 h (Fig. 2A). ASTX significantly inhibited the induction of α-SMA at 3 and 12 h and Col1A1 at 12 h of TGFβ1 stimulation. Induction of the fibrogenic genes by TGFβ1 was significantly inhibited by 10 and 25 μM of ASTX (Fig. 2B). Based on this finding, ASTX treatment for 12 h at 25 μM was chosen for the rest of the study.

ASTX did not alter the basal expression levels of α-SMA and Col1A1 mRNA in LX-2 cells, but significantly attenuated TGFβ1-induced expression of these genes (Fig. 3A). ASTX also significantly decreased the protein levels of α-SMA that were induced by TGFβ1 (Fig. 3B and C).

3.3. Smad3 played a major role in the induction of fibrogenic genes by TGFβ1 in LX-2 cells

As Smad3 is known to mediate TGFβ1 signaling for fibrogenic responses [37], we determined if Smad3 is involved in the repressive effect of ASTX on the induction of fibrogenic genes by TGFβ1. In the LX-2 cells transfected with scrambled control, the induction of fibrogenic genes by TGFβ1 was attenuated by ASTX (Fig. 4). When Smad3 was knocked down by ~80%, the basal mRNA levels of α-SMA and Col1A1, but not TGFβ1, were significantly decreased compared with scrambled control. TGFβ1 did not induce the expression of α-SMA and Col1A1 but its own mRNA levels were not altered when Smad3 was deficient.

3.4. ASTX attenuated phosphorylation and nuclear translocation of Smad3 in LX-2 cells

As the anti-fibrogenic effect of ASTX is likely mediated via Smad3, whether ASTX can inhibit Smad3 activation, i.e., phosphorylation and nuclear translocation, was evaluated in LX-2 cells. TGFβ1 stimulation markedly increased the levels of phosphorylated Smad3 at 30 min and ASTX treatment significantly inhibited the TGFβ1-induced phosphorylation (Fig. 5A). Smad3 phosphorylation is an important determinant of its nuclear translocation [38]. Consistent with the reduction in phosphorylated Smad3 by ASTX, the nuclear translocation of Smad3 was also reduced by ASTX, whereas TGFβ1 treatment increased nuclear Smad3

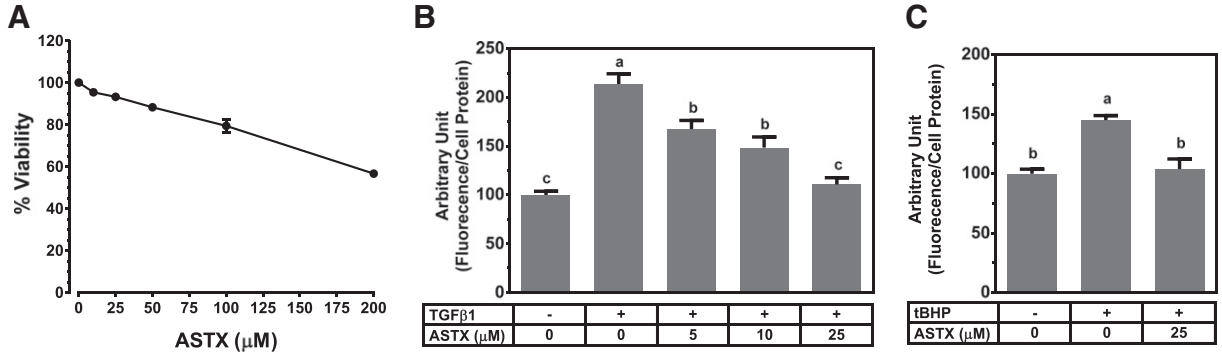

Fig. 1. ASTX repressed ROS production in LX-2 cells. (A) LX-2 cells were treated with 0–200 μM ASTX for 24 h for cytotoxicity measurement. Data are shown as mean ± SEM. n = 5. LX-2 cells were pretreated with 0, 5, 10 or 25 μM ASTX for 24 h, and subsequently they were exposed to 2 ng/mL TGFβ1 (B) or 10 μM tBHP (C) in the presence of ASTX for 24 h. Data are shown as mean ± SEM. n = 6–9. Bars sharing a common letter are not significantly different from each other ($P < 0.05$).

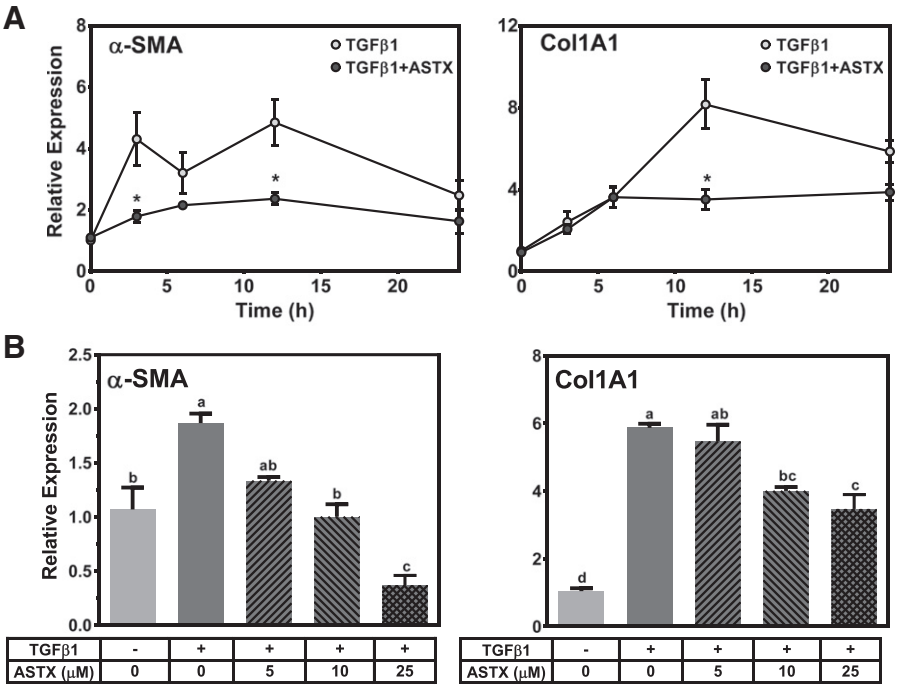

Fig. 2. ASTX repressed fibrogenic gene expression in a time- and dose-dependent manner in LX-2 cells. (A) LX-2 cells were pretreated with or without 25 μM ASTX for 24 h, after which they were exposed to 2 ng/mL TGFβ1 for 0–24 h. qRT-PCR was conducted to measure fibrogenic gene expression. Data are shown as mean ± SEM. n = 6. (B) LX-2 cells were pretreated with 0, 5, 10 or 25 μM ASTX for 24 h, then exposed to 2 ng/mL TGFβ1 for 24 h in the presence of the same ASTX concentration to conduct qRT-PCR. Data are shown as mean ± SEM. n = 6. Bars sharing a common letter are not significantly different from each other ($P < 0.05$).

levels (Fig. 5B). The activation of Smad3 requires other players in transducing TGFβ1 signaling. Upon TGFβ1 binding to TβRII, the receptor activates TβRI, which in turn phosphorylates Smad2 and Smad3 [15]. The phosphorylation of Smad2 and Smad3 allows them to complex with Smad4 for nuclear translocation. Smad7, transcriptionally induced by Smad3, is known to interact with TβRI through its carboxyl-terminal Mad homology 2 domains and therefore competes with Smad3 for binding to TβRI [39]. We found that the mRNA levels of Smad2, Smad3, Smad4, and Smad7 were significantly increased by TGFβ1 (Fig. 5C). However, the increase was abolished or significantly attenuated by ASTX except Smad4. Furthermore, ASTX almost completely abolished the TGFβ-induced increases in mRNA levels of both TβRI and TβRII.

3.5. ASTX prevented α-SMA elevation during activation of mouse primary HSCs

To gain insight into the role of ASTX in the early activation of quiescent HSCs, primary HSCs isolated from C57BL/6J mice were cultured on untreated petri dishes for 4 or 6 days for activation [40], with the addition of ASTX at day 2 or day 4, respectively. In the absence of ASTX, the expression of α-SMA, a prominent marker for the activation of quiescent HSCs, was significantly increased with time. The addition of ASTX for 2 days during the HSC activation significantly reduced α-SMA mRNA levels (Fig. 6A). At day 4 of incubation, the protein levels of α-SMA were increased, whereas the addition of ASTX for 2 days markedly decreased the protein levels (Fig. 6B). Compared with control cells cultured without ASTX for 6 days, ASTX treatment at days 0, 2, and 4 decreased α-SMA protein by 30–40% (Fig. 6C).

4. Discussion

The prevalence of NAFLD has reached 20% of the general population [41] and 30–80% of the obese population in the U.S. [42]. In obesity, increased flux of free fatty acids from hypertrophied adipocytes into the liver leads to oxidative stress and hepatocyte damage [4], which can stimulate Kupffer cells to secret pro-fibrogenic cytokines such as TGFβ1 that can activate HSCs [15]. Under the condition of chronic liver injury, sustained activation of HSCs results in excessive deposition of extracellular matrix, leading to the development of fibrosis [43]. Therefore, identification of anti-fibrogenic agents that can inhibit HSC activation may effectively lower the risk of hepatic fibrosis. In the present study, we demonstrated that ASTX represses the expression of TGFβ1-induced fibrogenic genes by inhibiting Smad3 activation in HSCs.

Chronic oxidative stress can lead to the development of hepatic fibrosis by stimulating proliferation and fibrogenic response in HSCs [44]. Free radicals and ROS are highly unstable, and react quickly with adjacent molecules, ultimately damaging nucleotides, proteins and lipids [45]. ASTX has been shown to be a potent ROS scavenger largely due to its unique molecular structure. The polar ends of ASTX allow it to quench electrons from free radicals and other oxidants, whereas a polyene chain can capture electron to terminate chain reaction [46]. In the present study, ASTX decreased cellular ROS levels induced by TGFβ1 or tBHP. The ROS reduction by ASTX may be achieved by scavenging radicals as it has been shown to scavenge peroxyl and hydroxyl radicals [46] and/or by interfering with signaling pathways that can lead to ROS production. It has been shown that TGFβ1 up-regulates NADPH oxidase 4 (NOX4), a key enzyme for ROS production in HSCs, and inhibition of TβRI activity reduces NOX4 expression and ROS production [47]. Therefore, our observation that ASTX decreased the expression of TβRI and other TGFβ signaling intermediates suggests that ASTX may potentially inhibit the upstream signal for NOX4 transcription, preventing ROS generation. In fact, ASTX decreased TGFβ1-induced NOX4 mRNA levels although it did not reach statistical significance ($P = 0.074$) (data not shown).

TGFβ1 is known to be the most potent pro-fibrogenic cytokine [37]. We observed that ASTX inhibits the TGFβ1-induced expression of fibrogenic genes, such as α-SMA and Col1A1. The expression of α-SMA is primarily regulated by Smad3 [48], whereas Col1A1 is known to be regulated by Smad3 [49] and specificity protein 1 (Sp1). In the present study, Smad3 knockdown by ~80% significantly decreased the basal expression of α-SMA and Col1A1, and TGFβ1 did

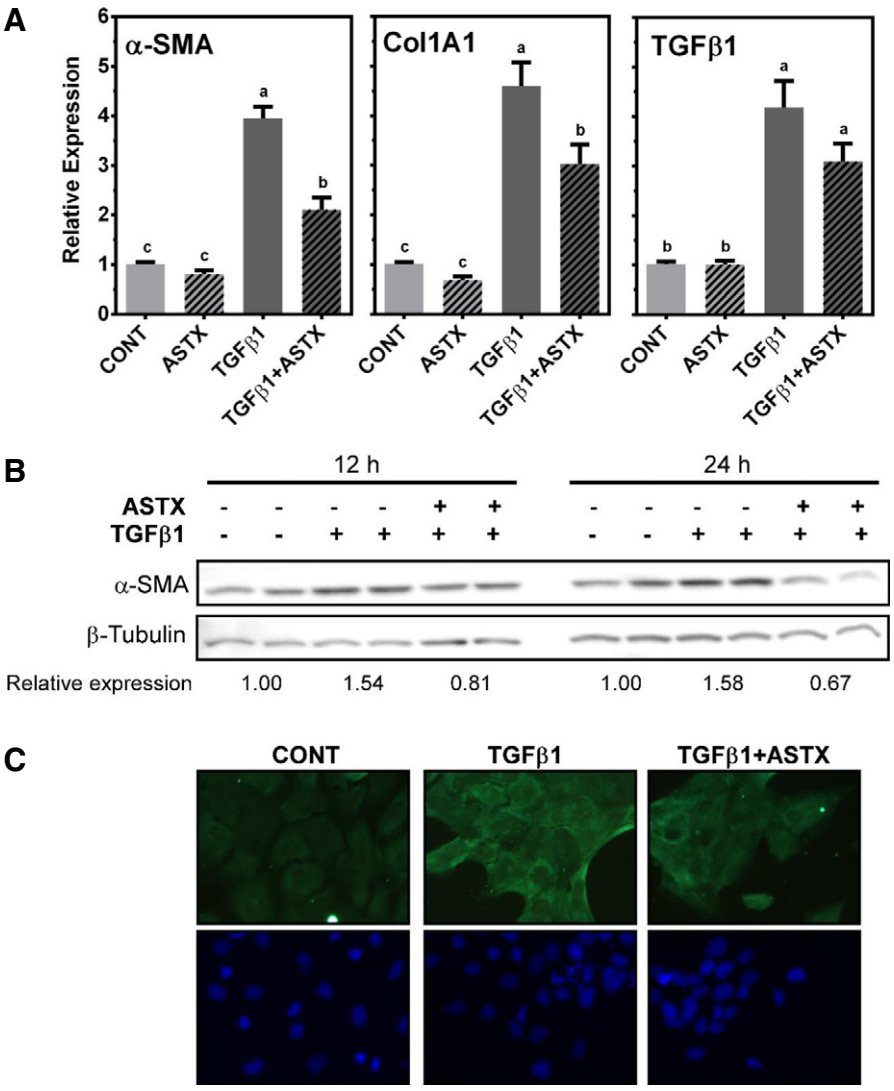

Fig. 3. ASTX repressed TGFβ1-induced fibrogenic gene expression in LX-2 cells. (A) LX-2 cells were pre-incubated with or without 25 μM ASTX for 24 h, and then stimulated with 2 ng/mL TGFβ1 in the presence or absence of ASTX for additional 24 h for qRT-PCR analysis. Control cells were harvested before TGFβ1 treatment. Data are shown as mean ± SEM. n = 9. Bars with a different letter are significantly different ($P < 0.05$). (B) LX-2 cells were pre-incubated with or without 25 μM ASTX for 24 h, and then stimulated with 2 ng/mL TGFβ1 in the presence or absence of ASTX for 12 or 24 h. Western blot analysis was conducted to measure α-SMA protein levels with using β-tubulin as a loading control. Representative blot image is show from 3 repeats. Densitometry analysis was conducted and averages of relative expression of α-SMA protein to control (no ASTX, no TGFβ1) are shown. (C) LX-2 cells were pre-incubated with or without 25 μM ASTX for 24 h, and subsequently they were stimulated with 2 ng/mL TGFβ1 with or without ASTX. Immunostaining of α-SMA protein is shown in green and DAPI staining is in blue.

not induce both gene expression when Smad3 was deficient. The data suggest that Smad3 plays a critical role in transducing TGFβ1 signaling for the induction of fibrogenic genes in HSCs. Although ASTX inhibited the TGFβ1-induced Col1A1 and α-SMA expression in the presence of functional Smad3, it had a minimal inhibitory effect on the expression of α-SMA in Smad3-deficient cells. This observation strengthens the notion that the inhibitory effect of ASTX on α-SMA and Col1A1 expression is likely mediated via Smad3. Other transcription factors, such as Krüppel-like factors (KLF) and CCAAT/enhancer binding protein β (CEBPβ), have also been shown to be involved in TGFβ1-induced fibrogenic gene expression [50]. However, the failure to induce α-SMA and Col1A1 expression by TGFβ1 when Smad3 is deficient strongly suggests that Smad3, but not KLF and CEBPβ, is the most critical transcription factor for the induction of the fibrogenic genes in response to TGFβ1 signaling in HSCs. ASTX also inhibited an increase in TGFβ1 mRNA by itself regardless of Smad3. Transcription of TGFβ1 has been suggested to be regulated mainly by Sp1 and KLF6 [51,52]. Therefore, ASTX may have a repressive effect on the activity of other TGFβ1-sensitive transcription factors in addition to Smad3.

Smad3 is one of the downstream effectors of TGFβ1 signaling that induces fibrogenesis in HSCs. Binding of TGFβ1 to TβRII, a cell surface TGFβ1 receptor, phosphorylates TβRI, which subsequently phosphorylates Smad2 and Smad3 for the induction of fibrogenic response [53]. In particular, Smad3 has been shown to be indispensable for TGFβ-induced fibrogenic gene expression [54]. Phosphorylation of Smad2 and Smad3 is required to make a complex with Smad4, which translocates to the nucleus for transcriptional induction [55]. In LX-2 cells, we observed that TGFβ1 induced the expression of Smad2, 3, and 7, TβRI and TβRII, which was attenuated by ASTX. The inhibitory action of ASTX in the expression of these intermediate effectors in TGFβ1 signaling may explain how ASTX prevents Smad3 activation, consequently inhibiting its target gene expression. Sp1 has been shown to transcriptionally regulate the expression of fibrogenic genes such as TGFβ1, Col1A1, TβRI, and TβRII [56]. The down-regulation of TGFβ1, TβRI and TβRII by ASTX in TGFβ1-stimulated LX-2 cells, as observed here, may suggest that ASTX may also inhibit Sp1. Studies have shown that Sp1 may cooperate with KLF6 to induce the transcription of TGFβ1, TβRI, and TβRII [50,52], and CEBPβ can also be activated by TGFβ1-triggered

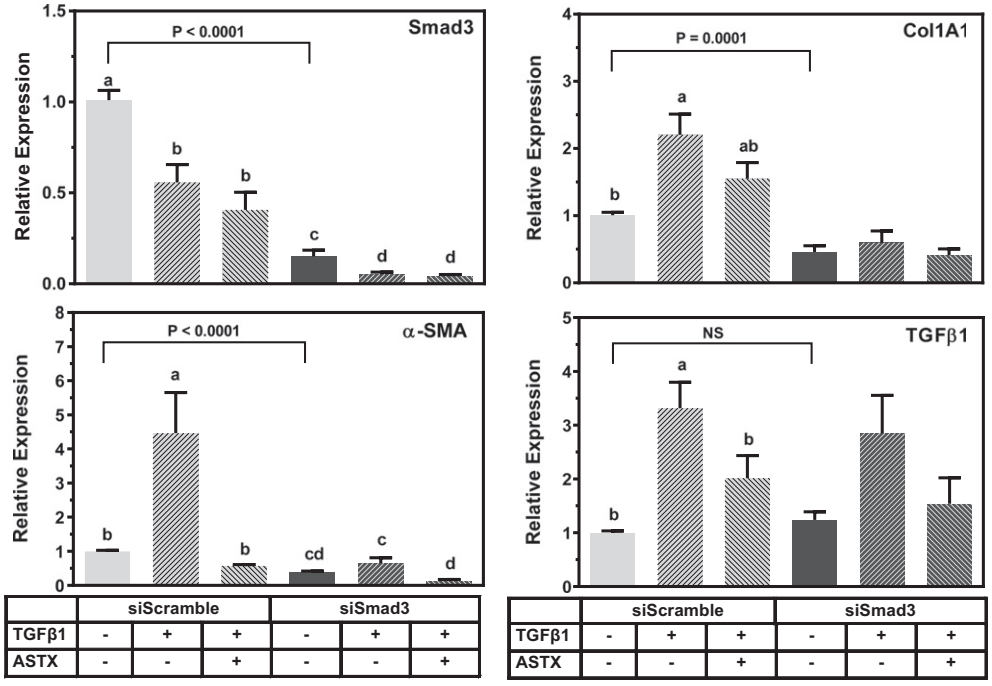

Fig. 4. Smad3 mediated TGFβ1-induced fibrogenic gene expression in LX-2 cells. LX-2 cells were transfected with Scramble control or Smad3 siRNA. Subsequently, they were pretreated with or without 25 μM ASTX for 12 h, after which they were activated by 2 ng/mL TGFβ1 for 12 h. qRT-PCR was used for data analyses. Data are shown as means ± SEM. n = 9. Bars sharing a common letter within the same siRNA treatment are not significantly different from each other (P < 0.05).

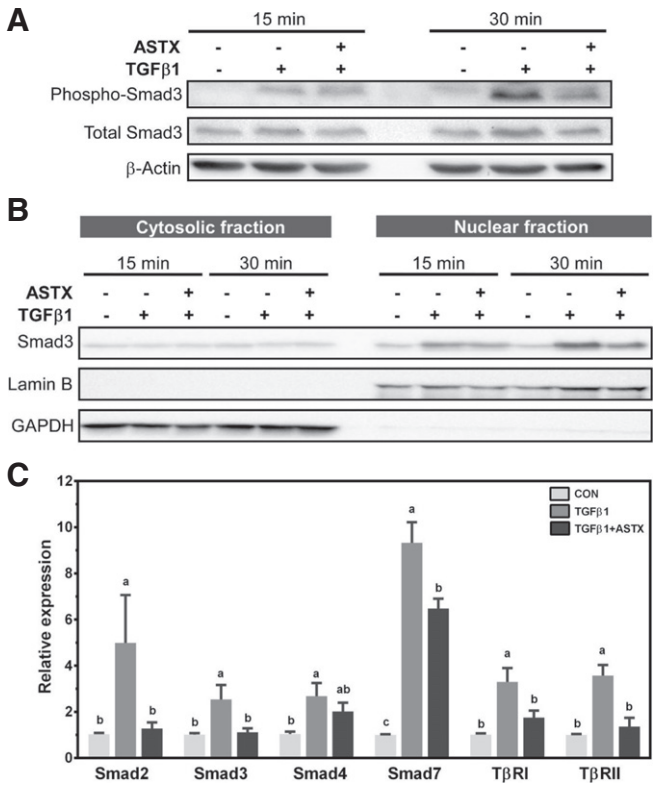

Fig. 5. ASTX attenuated TGFβ signaling for the activation of Smad3 in LX-2 cells. LX-2 cells were pre-incubated with or without 25 μM ASTX for 24 h and subsequently for additional 3 h with replenishing ASTX in the media. Subsequently, the cells were stimulated with 2 ng/mL TGFβ1 for 15 or 30 min to conduct Western blot for total and phosphorylated Smad3 (A) or to measure Smad3 protein in the cytoplasm and nucleus (B). Lamin B and GAPDH were used as a marker for nucleus and cytoplasm, respectively. (C) LX-2 cells were pre-incubated with 25 μM ASTX for 24 h, then stimulated with 2 ng/mL TGFβ1 for 12 h for qRT-PCR analysis. Data are shown as mean ± SEM. n = 9. Bars sharing a common letter are not significantly different from each other (P < 0.05).

ROS accumulation to induce the transcription of Col1A1. Further investigation is needed to establish the roles of Sp1, KLF6 and CEBPβ in modulating the anti-fibrogenic effect of ASTX.

Although the present study supports that ASTX decreases fibrogenic gene expression in HSCs by inhibiting Smad3 activation possibly via the inhibition of TGFβ receptors, it still remains elusive how ASTX inhibits TGFβ signaling. A potential explanation may involve a unique alignment of ASTX in phospholipid bilayers [19]. Although the intracellular distribution of ASTX in different organelles has not yet been fully investigated, it is likely that ASTX is embedded in cellular membranes, including plasma, mitochondrial, and nuclear membranes [57]. A study showed that integration of ASTX into an in vitro assembled membrane maintains the membrane integrity, whereas other carotenoids, such as β-carotene and lycopene, disrupt the membrane structure [58]. Accumulation of ASTX in cell membrane may thus alter membrane fluidity, affecting protein to protein interactions. Both TβRI and TβRII are transmembrane proteins located in the plasma membrane, while TGFβ signal transduction requires recruitment of TβRI to TβRII [59]. Therefore, it can be presumed that ASTX may inhibit TGFβ1 signal transduction by blocking the recruitment of TβRI to TβRII, resulting in decreased Smad3 phosphorylation and subsequent nuclear translocation. Future studies are warranted to test this possibility.

LX-2 cells are a good HSC model that is commonly used to evaluate TGFβ1-induced fibrogenic responses [40]. However, as LX-2 cells are somewhat activated HSCs as demonstrated by the high proliferation rate and lack of cytoplasmic lipid droplets [60], they are not well suited for evaluating the early stage activation of quiescent HSCs. Therefore, we additionally used primary mouse HSCs to gain insight into the effect of ASTX on the early stage of HSC activation. Primary quiescent HSCs are activated when cultured on an untreated plastic dish up to 7 days [61]. During the activation, quiescent HSCs are transdifferentiated into highly proliferative, myoblast-like cells that are characterized by the loss of lipid droplets and high α-SMA expression, an activation marker [62]. We found that when primary HSCs were incubated with ASTX during their activation, α-SMA mRNA and protein levels were markedly decreased, indicating that ASTX prevents the early stage activation of quiescent HSCs. This is a novel finding and requires further work to

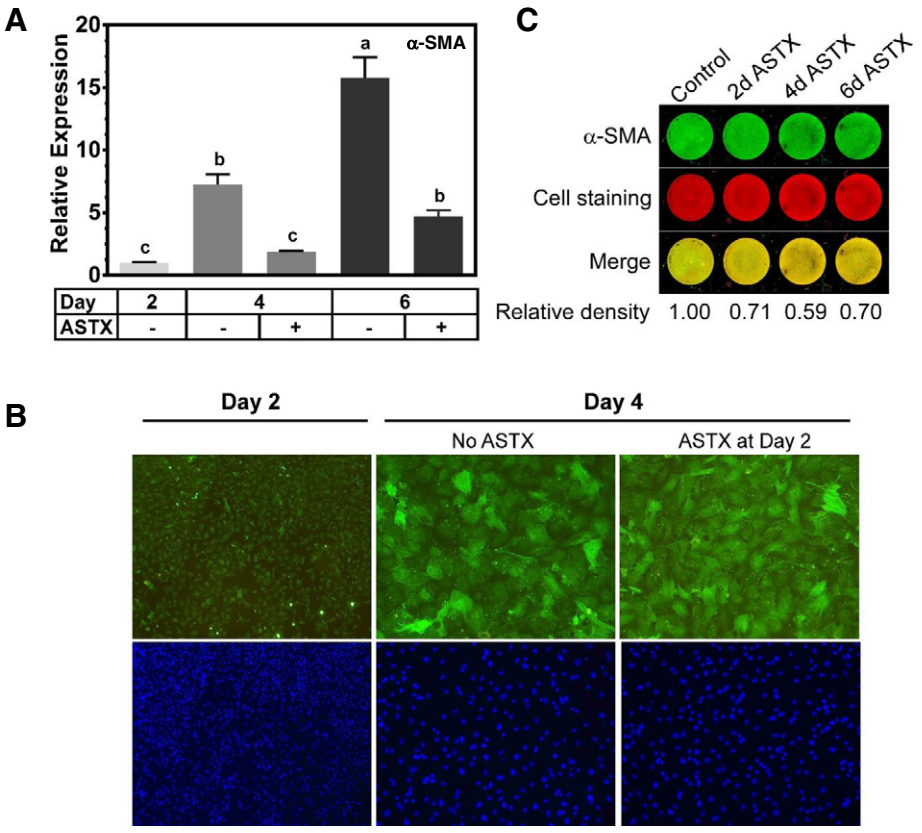

Fig. 6. ASTX inhibited the activation of quiescent mouse primary HSCs. (A) Primary HSCs were isolated from C57BL/6J mice and cultured on an untreated plastic dish for 6 days for activation. ASTX at 25 μM was added to cell medium at day 2 or day 4 for additional 2 days. Data are shown as mean ± SEM. n = 3. Bars sharing a common letter are not significantly different ($P < 0.05$). (B) Primary HSCs were cultured for 4 days for activation with addition of 25 μM ASTX at day 2 for 2 additional days. *Upper panel*, immunostaining of α-SMA. *Lower panel*, DAPI staining. (C) Primary HSCs were co-incubated with ASTX from day 0, 2 or 4 till day 6. In-cell Western was conducted to measure α-SMA protein levels. α-SMA protein is shown in green and total cell staining for cell number normalization is shown in red. The bottom panel shows the merging of α-SMA and total cell stain.

investigate the mechanisms underlying the inhibitory effect of ASTX on the activation of quiescent HSCs.

In conclusion, the present study, using both LX-2 and primary mouse HSCs, provides the first evidence that ASTX possesses anti-fibrogenic properties and prevents the early stage activation of quiescent HSCs. The inhibitory effect of ASTX on the expression of pro-fibrogenic mediators is attributable in part to the inhibition of the TGFβ1–Smad3 signaling pathway as evidenced by the attenuation of TGFβ1-induced Smad3 phosphorylation and nuclear translocation by ASTX. Further studies are warranted to investigate the mechanisms whereby ASTX inhibits TGFβ signaling in HSCs. Nonetheless, our findings here suggest that ASTX may potentially be used as a dietary means of lowering the risk of NAFLD and hepatic fibrosis in particular.

Acknowledgements

This work was supported by USDA AFRI 2012-67018-19290 to J. Lee and USDA Multi-state/Hatch CONS00916 to S. I. Koo and J. Lee.

References

[1] M. Lazo, J.M. Clark, The epidemiology of nonalcoholic fatty liver disease: a global perspective, Semin. Liver Dis. 28 (2008) 339–350.
[2] J.P. Ong, Z.M. Younossi, Epidemiology and natural history of NAFLD and NASH, Clin. Liver Dis. 11 (2007) 1–16.
[3] Y.-S. Lim, W.R. Kim, The global impact of hepatic fibrosis and end-stage liver disease, Clin. Liver Dis. 12 (2008) 733–746.
[4] J.K. Reddy, M.S. Rao, Lipid metabolism and liver inflammation. II. Fatty liver disease and fatty acid oxidation, Am. J. Physiol. Gastrointest. Liver Physiol. 290 (2006) G852–G858.
[5] J. Ludwig, T.R. Viggiano, D.B. McGill, B.J. Oh, Nonalcoholic steatohepatitis: Mayo Clinic experiences with a hitherto unnamed disease, Mayo Clin. Proc. 55 (1980) 434–438.
[6] E.M. Brunt, Pathology of nonalcoholic steatohepatitis, Hepatol. Res. 33 (2005) 68–71.
[7] E.E. Powell, W.G. Cooksley, R. Hanson, J. Searle, J.W. Halliday, L.W. Powell, The natural history of nonalcoholic steatohepatitis: a follow-up study of forty-two patients for up to 21 years, Hepatology 11 (1990) 74–80.
[8] A.J. Sanyal, C. Campbell-Sargent, F. Mirshahi, W.B. Rizzo, M.J. Contos, R.K. Sterling, V.A. Luketic, M.L. Shiffman, J.N. Clore, Nonalcoholic steatohepatitis: association of insulin resistance and mitochondrial abnormalities, Gastroenterology 120 (2001) 1183–1192.
[9] M. Ekstedt, L.E. Franzén, U.L. Mathiesen, L. Thorelius, M. Holmqvist, G. Bodemar, S. Kechagias, Long-term follow-up of patients with NAFLD and elevated liver enzymes, Hepatology 44 (2006) 865–873.
[10] G. Vernon, A. Baranova, Z.M. Younossi, Systematic review: the epidemiology and natural history of non-alcoholic fatty liver disease and non-alcoholic steatohepatitis in adults, Aliment. Pharmacol. Ther. 34 (2011) 274–285.
[11] V. Hernandez-Gea, S.L. Friedman, Pathogenesis of liver fibrosis, Annu. Rev. Pathol. 6 (2011) 425–456.
[12] S.L. Friedman, Stellate cell activation in alcoholic fibrosis—an overview, Alcohol. Clin. Exp. Res. 23 (1999) 904–910.
[13] M. Parola, G. Robino, Oxidative stress-related molecules and liver fibrosis, J. Hepatol. 35 (2001) 297–306.
[14] E. Williams, J. Iredale, Hepatic regeneration and TGF-β: growing to a prosperous perfection, Gut 46 (2000) 593–594.
[15] S.L. Friedman, Mechanisms of disease: mechanisms of hepatic fibrosis and therapeutic implications, Nat. Clin. Pract. Gastroenterol. Hepatol. 1 (2004) 98–105.
[16] J. Gauldie, P. Bonniaud, P. Sime, K. Ask, M. Kolb, TGF-beta, Smad3 and the process of progressive fibrosis, Biochem. Soc. Trans. 35 (2007) 661–664.
[17] I. Higuera-Ciapara, L. Felix-Valenzuela, F.M. Goycoolea, Astaxanthin: a review of its chemistry and applications, Crit. Rev. Food Sci. Nutr. 46 (2006) 185–196.
[18] G. Hussein, U. Sankawa, H. Goto, K. Matsumoto, H. Watanabe, Astaxanthin, a carotenoid with potential in human health and nutrition, J. Nat. Prod. 69 (2005) 443–449.
[19] F.J. Pashkow, D.G. Watumull, C.L. Campbell, Astaxanthin: a novel potential treatment for oxidative stress and inflammation in cardiovascular disease, Am. J. Cardiol. 101 (2008) 58D–68D.
[20] H.D. Choi, J.H. Kim, M.J. Chang, Y. Kyu-Youn, W.G. Shin, Effects of astaxanthin on oxidative stress in overweight and obese adults, Phytother. Res. 25 (2011) 1813–1818.

[21] K. Ohgami, K. Shiratori, S. Kotake, T. Nishida, N. Mizuki, K. Yazawa, S. Ohno, Effects of astaxanthin on lipopolysaccharide-induced inflammation in vitro and in vivo, Invest. Ophthalmol. Vis. Sci. 44 (2003) 2694–2701.
[22] G. Hussein, M. Nakamura, Q. Zhao, T. Iguchi, H. Goto, U. Sankawa, H. Watanabe, Antihypertensive and neuroprotective effects of astaxanthin in experimental animals, Biol. Pharm. Bull. 28 (2005) 47–52.
[23] K. Uchiyama, Y. Naito, G. Hasegawa, N. Nakamura, J. Takahashi, T. Yoshikawa, Astaxanthin protects beta-cells against glucose toxicity in diabetic db/db mice, Redox Rep. 7 (2002) 290–293.
[24] W. Li, A. Hellsten, L.S. Jacobsson, H.M. Blomqvist, A.G. Olsson, X.M. Yuan, Alpha-tocopherol and astaxanthin decrease macrophage infiltration, apoptosis and vulnerability in atheroma of hyperlipidaemic rabbits, J. Mol. Cell. Cardiol. 37 (2004) 969–978.
[25] Y. Yang, J.M. Seo, A. Nguyen, T.X. Pham, H.J. Park, Y. Park, B. Kim, R.S. Bruno, J. Lee, Astaxanthin-rich extract from the green alga *Haematococcus pluvialis* lowers plasma lipid concentrations and enhances antioxidant defense in apolipoprotein E knockout mice, J. Nutr. 141 (2011) 1611–1617.
[26] R. Weiskirchen, A.M. Gressner, Isolation and Culture of Hepatic Stellate Cells, vol. 1172005. 99–113.
[27] Y. Kamada, K. Mori, H. Matsumoto, S. Kiso, Y. Yoshida, S. Shinzaki, N. Hiramatsu, M. Ishii, K. Moriwaki, N. Kawada, T. Takehara, E. Miyoshi, N-Acetylglucosaminyltransferase V regulates TGF-β response in hepatic stellate cells and the progression of steatohepatitis, Glycobiology 22 (2012) 778–787.
[28] J.M. Graham, Fractionation of hepatic nonparenchymal cells, ScientificWorldJournal 2 (2002) 1347–1350.
[29] Y. Yang, Y. Park, D.A. Cassada, D.D. Snow, D.G. Rogers, J. Lee, In vitro and in vivo safety assessment of edible blue-green algae, *Nostoc commune* var. *sphaeroides* Kützing and *Spirulina plantensis*, Food Chem. Toxicol. 49 (2011) 1560–1564.
[30] S.G. Lee, B. Kim, Y. Yang, T.X. Pham, Y.K. Park, J. Manatou, S.I. Koo, O.K. Chun, J.Y. Lee, Berry anthocyanins suppress the expression and secretion of proinflammatory mediators in macrophages by inhibiting nuclear translocation of NF-kappaB independent of NRF2-mediated mechanism, J. Nutr. Biochem. 25 (4) (2013) 404–411.
[31] Y.K. Park, H.E. Rasmussen, S.J. Ehlers, K.R. Blobaum, F. Lu, V.L. Schlegal, T.P. Carr, J.Y. Lee, Repression of proinflammatory gene expression by lipid extract of *Nostoc commune* var *sphaeroides* Kutzing, a blue-green alga, via inhibition of nuclear factor-kappaB in RAW 264.7 macrophages, Nutr. Res. 28 (2008) 83–91.
[32] H.E. Rasmussen, K.R. Blobaum, Y.K. Park, S.J. Ehlers, F. Lu, J.Y. Lee, Lipid extract of *Nostoc commune* var. *sphaeroides* Kutzing, a blue-green alga, inhibits the activation of sterol regulatory element binding proteins in HepG2 cells, J. Nutr. 138 (2008) 476–481.
[33] C.S. Ku, T.X. Pham, Y. Park, B. Kim, M.S. Shin, I. Kang, J. Lee, Edible blue-green algae reduce the production of pro-inflammatory cytokines by inhibiting NF-κB pathway in macrophages and splenocytes, Biochim. Biophys. Acta Gen. Subj. 1830 (2013) 2981–2988.
[34] P. Angulo, Nonalcoholic fatty liver disease, N. Engl. J. Med. 346 (2002) 1221–1231.
[35] V. Proell, I. Carmona-Cuenca, M. Murillo, H. Huber, I. Fabregat, W. Mikulits, TGF-beta dependent regulation of oxygen radicals during transdifferentiation of activated hepatic stellate cells to myofibroblastoid cells, Comp. Hepatol. 6 (2007) 1.
[36] M. Guerin, M.E. Huntley, M. Olaizola, *Haematococcus* astaxanthin: applications for human health and nutrition, Trends Biotechnol. 21 (2003) 210–216.
[37] X. Liu, H. Hu, J.Q. Yin, Therapeutic strategies against TGF-beta signaling pathway in hepatic fibrosis, Liver Int. 26 (2006) 8–22.
[38] Y. Inagaki, R. Higashiyama, K. Higashi, Novel anti-fibrotic modalities for liver fibrosis: molecular targeting and regenerative medicine in fibrosis therapy, J. Gastroenterol. Hepatol. 27 (Suppl. 2) (2012) 85–88.
[39] R.P. Nagarajan, J. Zhang, W. Li, Y. Chen, Regulation of Smad7 promoter by direct association with Smad3 and Smad4, J. Biol. Chem. 274 (1999) 33412–33418.
[40] L. Xu, A.Y. Hui, E. Albanis, M.J. Arthur, S.M. O'Byrne, W.S. Blaner, P. Mukherjee, S.L. Friedman, F.J. Eng, Human hepatic stellate cell lines, LX-1 and LX-2: new tools for analysis of hepatic fibrosis, Gut 54 (2005) 142–151.
[41] M. Lazo, R. Hernaez, M.S. Eberhardt, S. Bonekamp, I. Kamel, E. Guallar, A. Koteish, F.L. Brancati, J.M. Clark, Prevalence of nonalcoholic fatty liver disease in the United States: the third national health and nutrition examination survey, 1988–1994, Am. J. Epidemol. 178 (2013) 38–45.
[42] S. Bellentani, F. Scaglioni, M. Marino, G. Bedogni, Epidemiology of non-alcoholic fatty liver disease, Dig. Dis. 28 (2010) 155–161.
[43] S. Weber, O.A. Gressner, R. Hall, F. Grünhage, F. Lammert, Genetic determinants in hepatic fibrosis: from experimental models to fibrogenic gene signatures in humans, Clin. Liver Dis. 12 (2008) 747–757.
[44] A. Galli, G. Svegliati-Baroni, E. Ceni, S. Milani, F. Ridolfi, R. Salzano, M. Tarocchi, C. Grappone, G. Pellegrini, A. Benedetti, C. Surrenti, A. Casini, Oxidative stress stimulates proliferation and invasiveness of hepatic stellate cells via a MMP2-mediated mechanism, Hepatology 41 (2005) 1074–1084.
[45] D.P. Jones, Radical-free biology of oxidative stress, Am. J. Physiol. Cell Physiol. 295 (2008) C849–C868.
[46] E. Rodrigues, L.R. Mariutti, A.Z. Mercadante, Scavenging capacity of marine carotenoids against reactive oxygen and nitrogen species in a membrane-mimicking system, Mar. Drugs 10 (2012) 1784–1798.
[47] P. Sancho, J. Mainez, E. Crosas-Molist, C. Roncero, C.M. Fernández-Rodriguez, F. Pinedo, H. Huber, R. Eferl, W. Mikulits, I. Fabregat, NADPH oxidase NOX4 mediates stellate cell activation and hepatocyte cell death during liver fibrosis development, PLoS ONE 7 (2012) e45285.
[48] B. Hu, Z. Wu, S.H. Phan, Smad3 mediates transforming growth factor-beta-induced alpha-smooth muscle actin expression, Am. J. Respir. Cell Mol. Biol. 29 (2003) 397–404.
[49] S. Kim, Y. Lee, J.E. Seo, K.H. Cho, J.H. Chung, Caveolin-1 increases basal and TGF-beta1-induced expression of type I procollagen through PI-3 kinase/Akt/mTOR pathway in human dermal fibroblasts, Cell. Signal. 20 (2008) 1313–1319.
[50] D.A. Mann, D.E. Smart, Transcriptional regulation of hepatic stellate cell activation, Gut 50 (2002) 891–896.
[51] V. Ellenrieder, TGFbeta regulated gene expression by Smads and Sp1/KLF-like transcription factors in cancer, Anticancer Res. 28 (2008) 1531–1539.
[52] Y. Kim, V. Ratziu, S.-G. Choi, A. Lalazar, G. Theiss, Q. Dang, S.-J. Kim, S.L. Friedman, Transcriptional activation of transforming growth factor β1 and its receptors by the Kruppel-like Factor Zf9/Core promoter-binding protein and Sp1: potential mechanisms for autocrine fibrogenesis in response to injury, J. Biol. Chem. 273 (1998) 33750–33758.
[53] A. Biernacka, M. Dobaczewski, N.G. Frangogiannis, TGF-beta signaling in fibrosis, Growth Factors 29 (2011) 196–202.
[54] A. LEASK, D.J. ABRAHAM, TGF-β signaling and the fibrotic response, FASEB J. 18 (2004) 816–827.
[55] K. Matsuzaki, Smad phosphoisoform signaling specificity: the right place at the right time, Carcinogenesis 32 (2011) 1578–1588.
[56] M. Centrella, C. Ji, S. Casinghino, T. McCarthy, Rapid flux in transforming growth factor-beta receptors on bone cells, J. Biol. Chem. 271 (1996) 18616–18622.
[57] K. Takahashi, M. Watanabe, T. Takimoto, Y. Akiba, Uptake and distribution of astaxanthin in several tissues and plasma lipoproteins in male broiler chickens fed a yeast (*Phaffia rhodozyma*) with a high concentration of astaxanthin, Br. Poult. Sci. 45 (2004) 133–138.
[58] H.P. McNulty, J. Byun, S.F. Lockwood, R.F. Jacob, R.P. Mason, Differential effects of carotenoids on lipid peroxidation due to membrane interactions: X-ray diffraction analysis, Biochim. Biophys. Acta 1768 (2007) 167–174.
[59] F. Huang, Y.G. Chen, Regulation of TGF-beta receptor activity, Cell Biosci. 2 (2012) 9.
[60] J. Herrmann, A.M. Gressner, R. Weiskirchen, Immortal hepatic stellate cell lines: useful tools to study hepatic stellate cell biology and function? J. Cell. Mol. Med. 11 (2007) 704–722.
[61] E. Guimaraes, J. Best, L. Dolle, M. Najimi, E. Sokal, L. van Grunsven, Mitochondrial uncouplers inhibit hepatic stellate cell activation, BMC Gastroenterol. 12 (2012) 68.
[62] H. Senoo, K. Yoshikawa, M. Morii, M. Miura, K. Imai, Y. Mezaki, Hepatic stellate cell (vitamin A-storing cell) and its relative—past, present and future, Cell Biol. Int. 34 (2010) 1247–1272.